Tetsuo Sasao and André B. Fletcher
Introduction to VLBI Systems
Chapter 1
Lecture Notes for KVN Students
Based on Ajou University Lecture Notes
(to be further edited)
Version 2.
Issued on February 28, 2005.
Revised on March 18, 2005.
Revised on February 4, 2006.

Basic Knowledge of Radio Astronomy

Contents

1 'Windows' for Ground–based Astronomy

Figure 1 shows how the Earth's atmosphere transmits electromagnetic waves from the Universe. The curve over the hatched area in this figure corresponds to the height in the atmosphere at which the radiation is attenuated by a factor of 1/2.

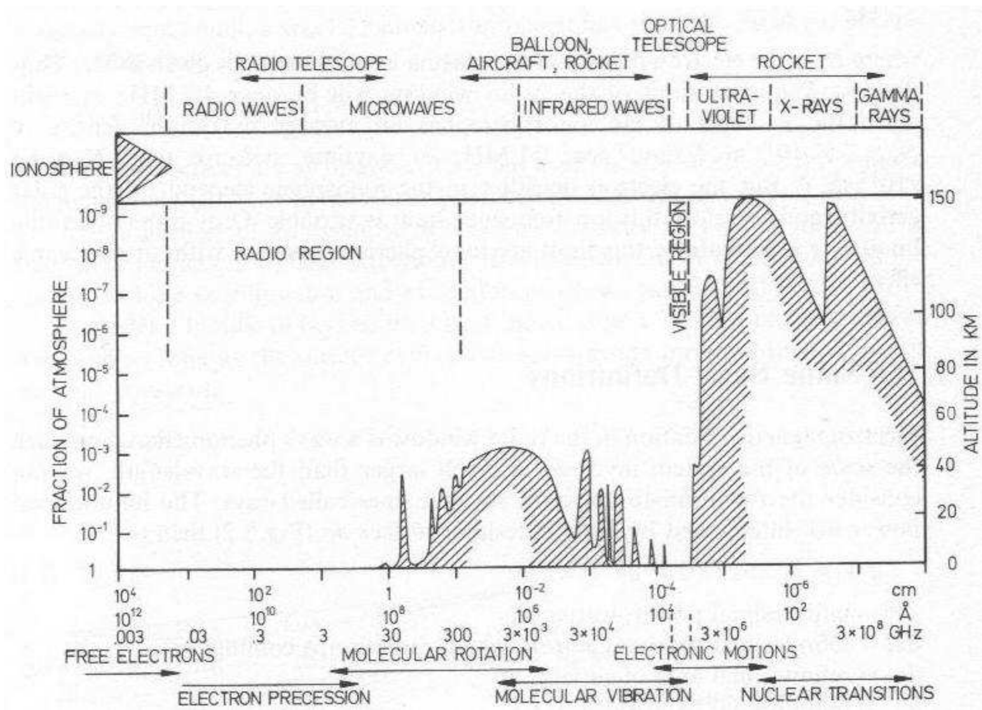

Figure 1: 'Windows' for ground-based astronomy (from Rohlfs & Wilson, 2001).

This figure shows that the Earth's atmosphere is largely transparent in the radio (15 MHz – 300 GHz) and visible light (360 THz – 830 THz) regions of the electromagnetic spectrum. These two regions are the main 'windows' for ground-based astronomical observations. VLBI (Very Long Baseline Interferometry) is one of the techniques used to observe astronomical radio sources through the 'radio window'.

2 Various Classifications of Astronomical Radio Sources

There are several ways to classify astronomical radio sources. Typical classifications are:

- - **Thermal source**
    Source emitting via a thermal mechanism (e.g. blackbody radiation),
  - **Non-thermal source**
    Source emitting via a non-thermal mechanism (e.g. synchrotron radiation, inverse Compton scattering, annihilation radiation, maser emission, etc.),
- - **Continuum source**
    Source emitting over a broad range of frequencies,
  - **Spectralline source**
    Source emitting in narrow lines at specific frequencies,

  and
- - **Galactic source**
    Source inside our Milky Way Galaxy,
  - **Extragalactic source**
    Source outside our Galaxy.

3 Spectra of Typical Continuum Radio Sources

Figure 2 shows typical spectra of continuum radio sources.
These spectra are characterized by a quantity called 'spectral index' α, defined by the formula: $\mathcal{S}_\nu \propto \nu^{-\alpha}$, where $\mathcal{S}_\nu$ is a quantity called the 'flux density' [unit: Jy (Jansky) $\equiv 10^{-26} W m^{-2} Hz^{-1}$], which is a measure of the strength of the radiation from a source.

Thermal and non–thermal sources usually show different spectral indices, namely:
$\alpha \cong -2$ for thermal sources,
and
$\alpha \geq 0$ for non-thermal sources.

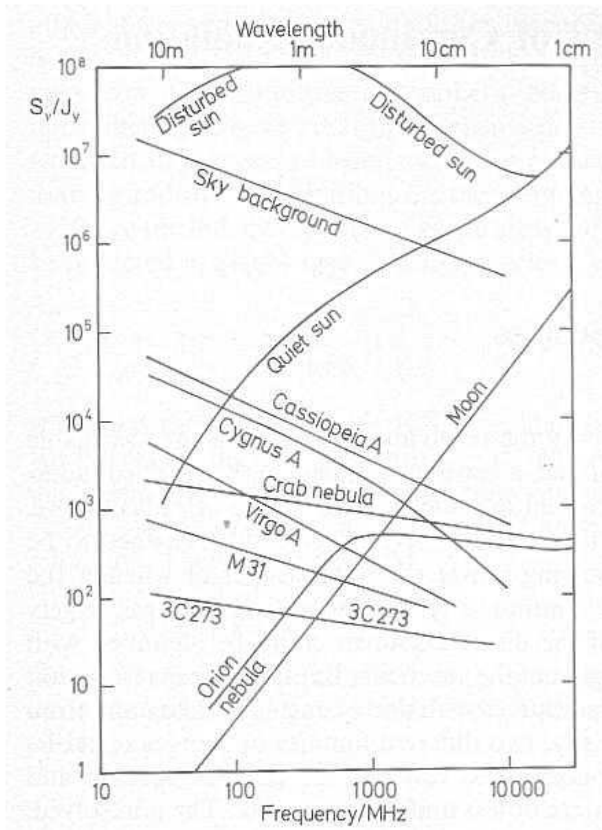

Figure 2: Spectra of galactic and extragalactic continuum radio sources (from Kraus, 1986).

4 Spectralline Radio Sources

An example of a thermal spectralline source showing many molecular lines is given in Figure 3.

Examples of spectra of non-thermal maser line sources obtained in test observations for the VERA (VLBI Exploration of Radio Astrometry) array in Japan are shown in Figures 4, 5, and 6.

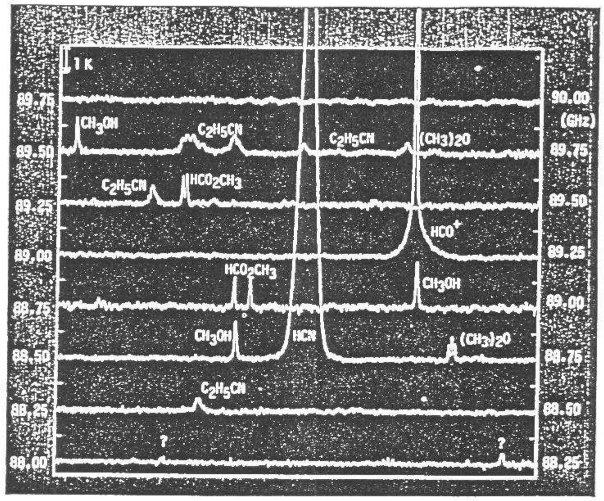

Figure 3: Thermal molecular lines observed in the Orion-KL star–forming region (Kaifu et al., 1985).

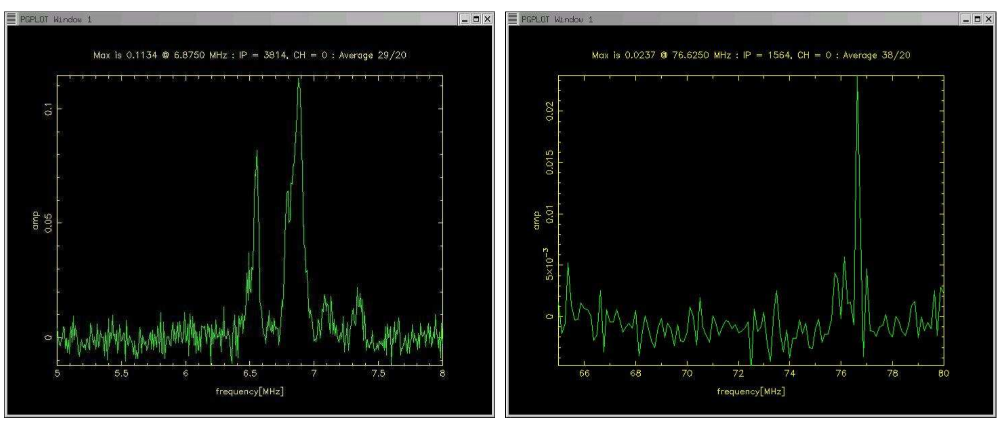

Figure 4: H_2O maser lines in Cep A (left), and RT Vir (right) (courtesy of VERA group, Japan, 2002).

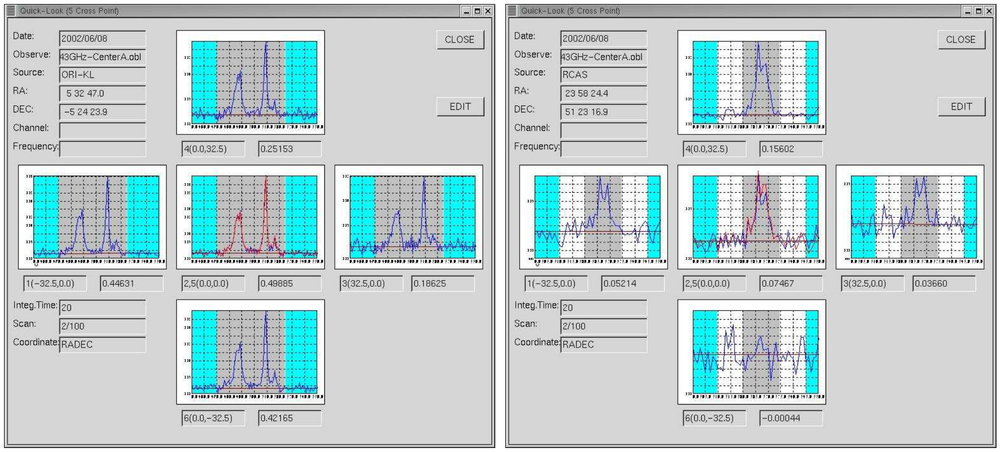

Figure 5: SiO maser lines in Orion-KL (left), and R Cas (right) observed in pointing tests for a VERA antenna (courtesy of VERA group, Japan, 2002).

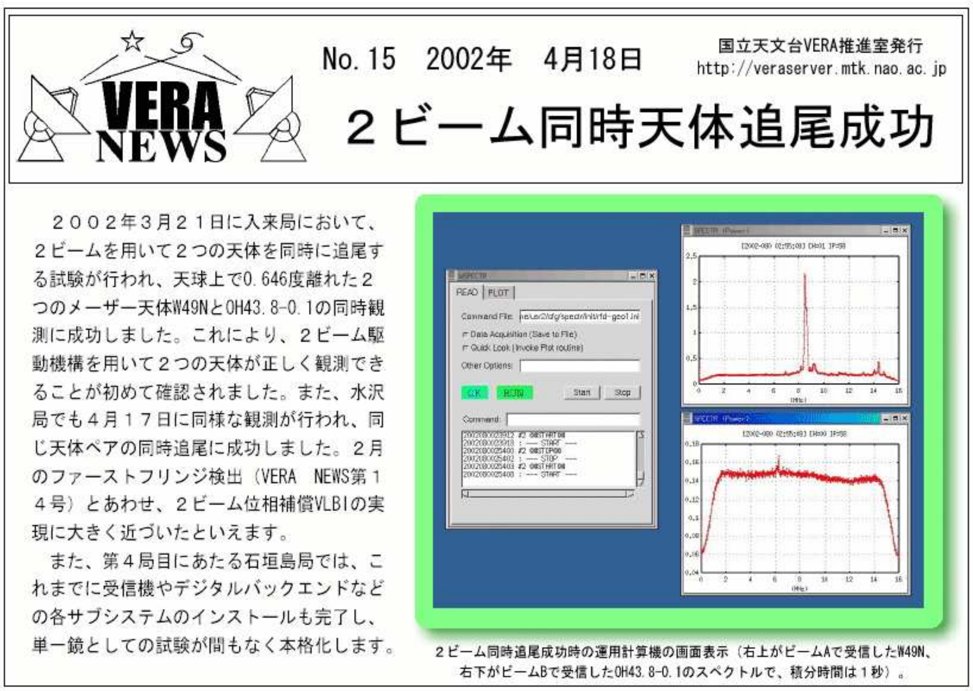

VERA NEWS

No. 15　2002年　4月18日

国立天文台VERA推進室発行
http://veraserver.mtk.nao.ac.jp

２ビーム同時天体追尾成功

２００２年３月２１日に入来局において、２ビームを用いて２つの天体を同時に追尾する試験が行われ、天球上で0.646度離れた２つのメーザー天体W49NとOH43.8-0.1の同時観測に成功しました。これにより、２ビーム駆動機構を用いて２つの天体が正しく観測できることが初めて確認されました。また、水沢局でも４月１７日に同様な観測が行われ、同じ天体ペアの同時追尾に成功しました。２月のファーストフリンジ検出（VERA　NEWS第１４号）とあわせ、２ビーム位相補償VLBIの実現に大きく近づいたといえます。

また、第４局目にあたる石垣島局では、これまでに受信機やデジタルバックエンドなどの各サブシステムのインストールも完了し、単一鏡としての試験が間もなく本格化します。

２ビーム同時追尾成功時の運用計算機の画面表示（右上がビームAで受信したW49N、右下がビームBで受信したOH43.8-0.1のスペクトルで、積分時間は１秒）。

Figure 6: H_2O maser lines in W49 N and OH43.8, observed simultaneously with a VERA dual-beam antenna (courtesy of VERA group, Japan, 2002).

5 Designations of Astronomical Radio Sources

There are many designation systems for naming radio sources. Examples are given in the following. As a result, radio sources are often identified by several different names.

- IAU 1974 system of designation ('IAU name', see, e.g., Explanatory Supplement to American Astronomical Almanac)
  - identifies a radio source by a six, seven, or eight-digit number, such as 0134+329, which tells us that the right ascension of the source is $01^h\ 34^m$, and its declination is $+32.^\circ9$ (usually in the B1950 equinox system).
  - sometimes source types or catalog acronyms are added, e.g., pulsars are called 'PSR0950+08', and sources from the Parkes Sky Survey as 'PKS1322-42'.
- 3C-name, 4C-name
  - identifies an extragalactic radio source by a serial number in the Third Cambridge Catalog, and by declination in the Fourth Cambridge Survey Catalog.
  - examples are 3C84, 3C273, 3C345, 4C39.25, etc.
- W-name
  - is based on Westerhout's (1958) catalog of HII regions.
  - examples are W49 N, W3(OH), W51 M, etc.

6 Designations of Frequency Bands

The basic unit of radio frequency is Hz (Hertz: cycle per second). In order to describe high frequency, typically used in radio astronomical observations or communications, we frequently use the following secondary units: kHz (kilohertz: 10^3 Hz), MHz (megahertz: 10^6 Hz), GHz (gigahertz: 10^9 Hz), and THz (terahertz: 10^{12} Hz).

Radio frequency bands used in astronomical observations, as well as in communications, are designated by one or a few alphabetic characters. Two systems of designations are shown in Figure 7.

In radio astronomy, IEEE STD-521-1976 designations have been used. Examples are:

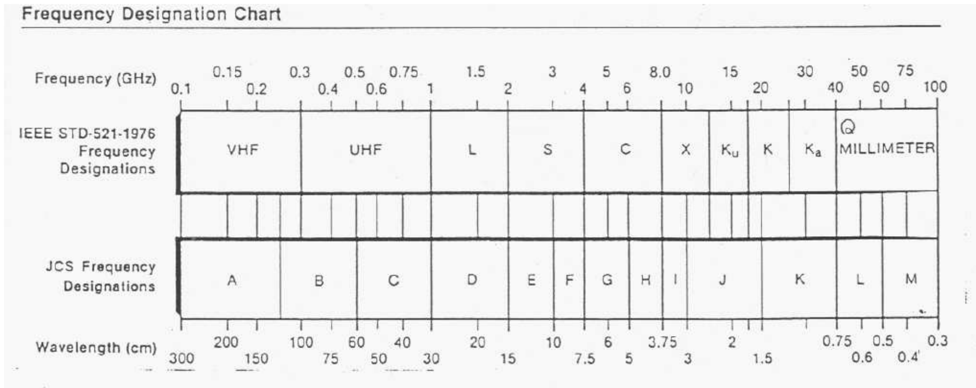

Figure 7: Frequency designations.

- L–band : GPS satellite, observations of OH masers,
- S– and X–bands : geodetic VLBI observations,
- K–band : observations of H_2O masers, and
- Q–band : observations of SiO masers.

7 Basic Quantities in Radio Astronomy

The following quantities are commonly used in radio astronomy to characterize radio waves coming from celestial bodies.

7.1 Intensity (Specific/Monochromatic Intensity) I_ν or Brightness B_ν

The intensity I_ν (or brightness B_ν) is the quantity of electromagnetic radiation energy incoming from a certain direction in the sky, per unit solid angle, per unit time, per unit area perpendicular to this direction, and per unit frequency bandwidth with center frequency ν. The SI unit of this specific (or monochromatic) intensity is thus: W m^{-2} Hz^{-1} sr^{-1} (Figure 8).

In terms of the monochromatic intensity I_ν, the power dW of radiation coming from a direction $\boldsymbol{s}$ within a solid angle $d\Omega$, through a cross-section of area $d\sigma$ with a normal inclined by an angle θ from the direction $\boldsymbol{s}$, within a frequency bandwidth $d\nu$ centered at ν, is given by:

$$dW = I_\nu(\boldsymbol{s}) \cos\theta \, d\Omega \, d\sigma \, d\nu. \tag{1}$$

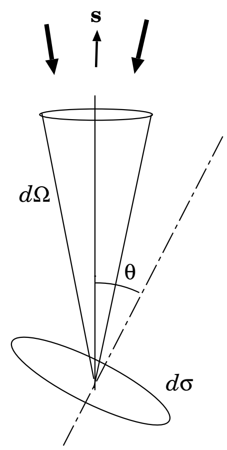

Figure 8: Definition of Specific/Monochromatic Intensity I_ν (or Brightness B_ν).

7.2 Constancy of the Monochromatic Intensity I_ν

The monochromatic intensity I_ν remains constant along a ray path, irrespective of the distance from the emitting source, as long as no absorption, emission, or scattering occurs along the path. An explanation of this constancy may be given as follows.

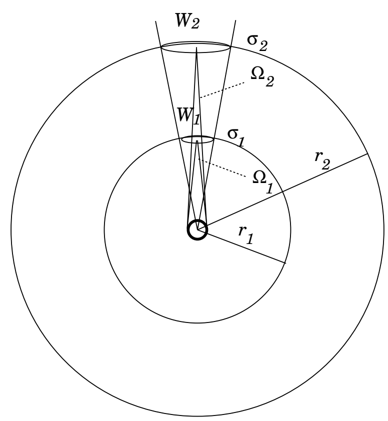

Figure 9: Constancy of the monochromatic intensity I_ν along the ray path.

Let us assume a spherically symmetric distribution of radiation from an emitting source at the center, without any intervening absorption, emission, or scattering, as shown in Figure 9. Let a cone-like ray tube of constant opening angle intersect a sphere of radius r, forming a cross–section of area σ, and let the source be seen to subtend a solid angle Ω at this radius. The power of the radiation with bandwidth $\Delta\nu$ passing through this cross–section is $W = I_\nu \, \Omega \, \sigma \Delta\nu$, which must be constant at any radius along the tube, as long as the radius is much larger than the source size. Now, the solid angle of the source Ω and the area of the cross–section σ vary as $\Omega \propto r^{-2}$ and $\sigma \propto r^2$, respectively. Therefore, the monochromatic intensity $I_\nu = W/(\Omega \, \sigma \, \Delta\nu)$ must be constant along the path.

7.3 'Spectral Flux Density' or 'Flux Density' or 'Flux' $\mathcal{S}_\nu$

The spectral flux density $\mathcal{S}_\nu$ is the quantity of radiation energy incoming through a cross section of unit area, per unit frequency bandwidth, and per unit time. A special unit called 'Jansky (Jy)' is widely used in radio astronomy for the spectral flux density. This unit is defined as: 1 Jy = 10^{-26} W m^{-2} Hz^{-1}.

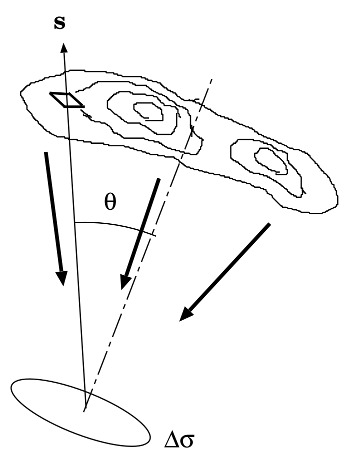

Figure 10: Definition of spectral flux density $\mathcal{S}_\nu$.

The spectral flux density $\mathcal{S}_\nu$ is related to the intensity I_ν by an integral over a solid angle Ω:

$$\begin{aligned} \mathcal{S}_\nu &= \iint_\Omega I_\nu(\boldsymbol{s}) \cos\theta \, d\Omega, \\ &= \iint_\Omega I_\nu(\theta, \phi) \, \cos\theta \, \sin\theta \, d\theta \, d\phi, \end{aligned} \tag{2}$$

where Ω could be, for example, a solid angle subtended by a radio source (see Figure 10).

7.4 Power/Energy/Radiation Flux Density $\mathcal{S}$

The power/energy/radiation flux density $\mathcal{S}$ is the quantity of radiation energy, over the whole frequency range, incoming through a cross section of unit area, per unit time. Therefore,

$$\mathcal{S} = \int_0^\infty \mathcal{S}_\nu \, d\nu. \tag{3}$$

When we are interested in the "received" power flux density only, we restrict the range of integration to the observing bandwidth $\Delta\nu$, i.e.,

$$\mathcal{S} = \int_{\Delta\nu} \mathcal{S}_\nu \, d\nu. \tag{4}$$

The unit of power flux density is: W m^{-2}.

7.5 Spectral Energy Density per Unit Solid Angle u_ν

The spectral energy density per unit solid angle, $u_\nu(\boldsymbol{s})$, is the volume density of the radiation energy incident from a certain direction $\boldsymbol{s}$, per unit solid angle, and per unit frequency bandwidth. The unit is J m^{-3} Hz^{-1} sr^{-1}.

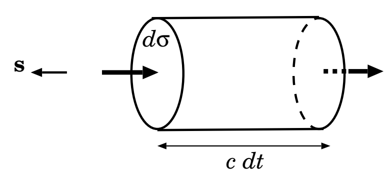

Figure 11: Radiation energy per unit solid angle in a tube.

Let us consider a cylindrical tube with a cross section of area $d\sigma$ perpendicular to the ray propagation direction, and with a length cdt, which is the distance travelled by the radiation during a time interval dt at light speed c ($= 2.998 \times 10^8$ m s^{-1}) (see Figure 11). The radiation energy dU_ν (J Hz^{-1} sr^{-1}) per unit solid angle, and per unit frequency bandwidth, contained in the cylinder may be expressed either in terms of the spectral energy density per unit solid angle, $u_\nu(\boldsymbol{s})$, or in terms of the intensity $I_\nu(\boldsymbol{s})$, as:

$$\begin{aligned} dU_\nu &= u_\nu(\boldsymbol{s}) \, cdt \, d\sigma, \\ dU_\nu &= I_\nu(\boldsymbol{s}) \, dt \, d\sigma. \end{aligned} \tag{5}$$

Therefore, these quantities are related to each other by:

$$I_\nu(\boldsymbol{s}) = c\, u_\nu(\boldsymbol{s}). \tag{6}$$

7.6 Spectral Energy Density U_ν

The spectral energy density U_ν is the volume density of the energy of the radiation, per unit frequency bandwidth, incoming from all directions (Figure 12).

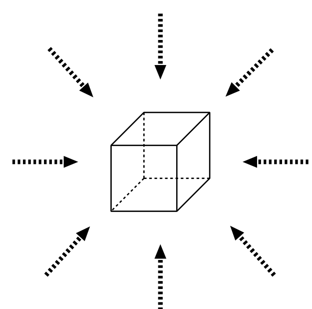

Figure 12: Spectral energy density: energy of radiation coming from all directions, contained in a unit volume.

Therefore,

$$U_\nu = \oint u_\nu(\boldsymbol{s}) d\Omega = \frac{1}{c} \oint I_\nu(\boldsymbol{s}) d\Omega. \tag{7}$$

The unit is J m^{-3} Hz^{-1}.

8 Emission and Absorption of Electromagnetic Radiation

8.1 Elementary Quantum Theory of Radiation (A. Einstein, 1916)

Let us consider a gaseous medium consisting of a large number of particles (atoms or molecules) of the same species. Let us also consider that each particle exists in one of the quantum states Z_1, Z_2, ..., with energy levels E_1, E_2, ... If $E_m < E_n$ for a pair of states Z_m and Z_n, a particle can absorb an amount of radiation energy $E_n - E_m$ in a transition from Z_m to Z_n. Also, a particle can emit the same amount of energy in a transition from

Z_n to Z_m (Figure 13). The frequency of the absorbed or emitted radiation is determined by the equation:

$$h\nu_{mn} = E_n - E_m, \tag{8}$$

where h is the Planck constant ($h = 6.626 \times 10^{-34}$ J s).

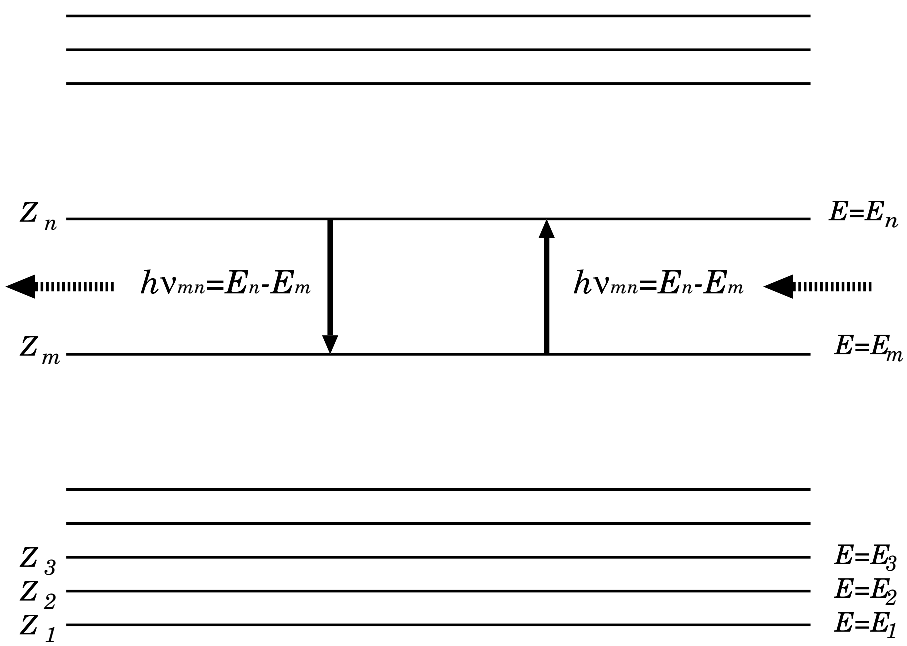

Figure 13: Energy levels and transitions with emission (left–hand arrow) or absorption (right–hand arrow) of radiation.

The energy levels here may be distributed continuously (continuum emission) or discretely (line emission). Note that even in the discrete level case, the frequency is spread over a finite 'line width', due to the Doppler shifts in randomly moving gaseous media in the universe.

Three kinds of transitions may occur between these two states (Figure 14), as follows:

(1) Spontaneous emission $\quad Z_n \rightarrow Z_m$

The spontaneous emission emerges due to a transition which occurs 'by itself', without any external influence (Figure 15). The probability df_{sp} for the spontaneous emission to occur within a small solid angle $d\Omega$ towards a direction -$\boldsymbol{s}$, within a small frequency bandwidth $d\nu$ around the frequency $\nu_{mn} = (E_n - E_m) / h$, and during a small time interval dt, must be proportional to $d\nu \, d\Omega \, dt$. Therefore, the probability can be expressed through a

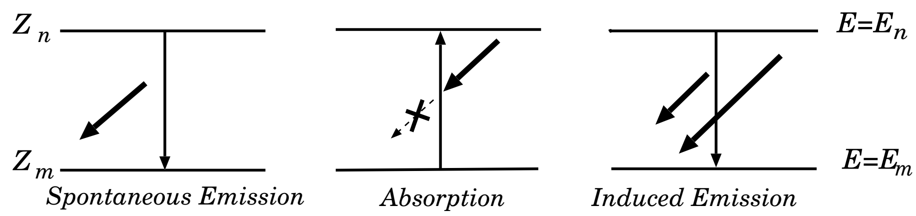

Figure 14: The three possible transitions between two energy states.

certain coefficient α_n^m as:

$$df_{sp} = \alpha_n^m \, d\nu \, d\Omega \, dt. \tag{9}$$

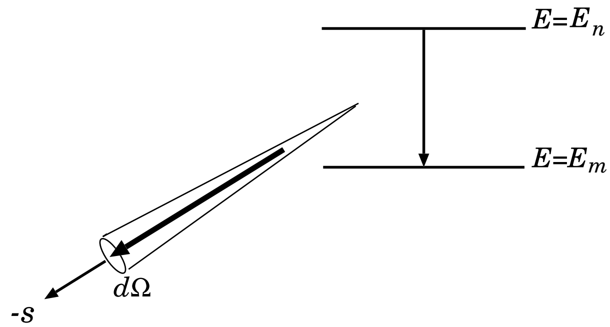

Figure 15: Spontaneous emission of radiation.

(2) Absorption $\qquad Z_m \rightarrow Z_n$

Some of the radiation passing through the gaseous medium may be absorbed in a transition from Z_m to Z_n, at a frequency around $\nu_{mn} = (E_n - E_m) \,/\, h$ (Figure 16). The absorption probability df_{ab} for the radiation incident from a direction within a small solid angle $d\Omega$ around $\boldsymbol{s}$, and in a small frequency bandwidth $d\nu$, during a short time interval dt, must be proportional to $d\nu \, d\Omega \, dt$ **and** to the spectral energy density per unit solid angle, $u_\nu(\boldsymbol{s})$, of the radiation itself. Therefore, introducing a proportionality coefficient β_m^n, we have:

$$df_{ab} = \beta_m^n \, u_\nu(\boldsymbol{s}) \, d\nu \, d\Omega \; dt. \tag{10}$$

(3) Induced (or stimulated) emission $\qquad Z_n \rightarrow Z_m$

Radiation with a frequency ν incident from a certain direction $\boldsymbol{s}$ may induce (or 'stimulate') transitions of gas particles from higher to lower energy

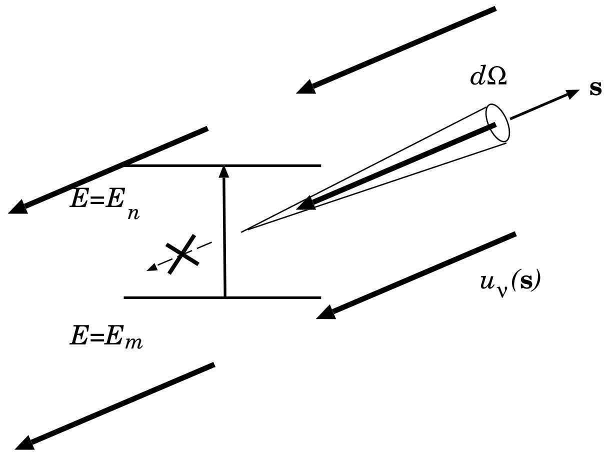

Figure 16: Absorption of radiation.

levels, such that the newly emitted radiation has the same frequency ν, and the same direction of propagation -$\boldsymbol{s}$, as the incident radiation (Figure 17). The probability df_{st} for the induced (or stimulated) emission to occur in a

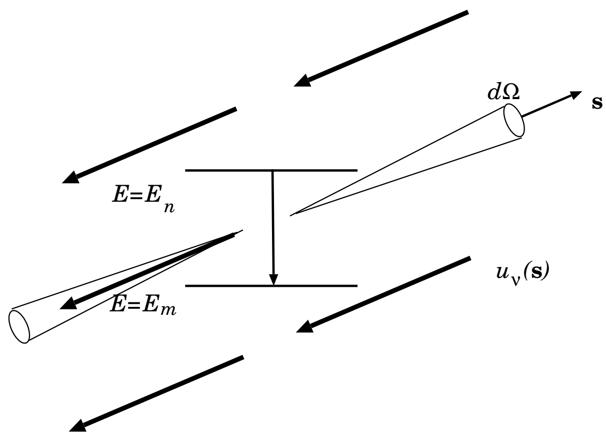

Figure 17: Induced (or stimulated) emission of radiation.

direction within a small solid angle $d\Omega$ around -$\boldsymbol{s}$, and in a small frequency bandwidth $d\nu$ around $\nu_{mn} = (E_n - E_m)\,/\,h$, during a short time interval dt, must be proportional to $d\nu\, d\Omega\, dt$ **and** to the spectral energy density per unit solid angle $u_\nu(\boldsymbol{s})$ of the incident radiation. Therefore, introducing a proportionality coefficient β_n^m, we have:

$$df_{st} = \beta_n^m \; u_\nu(\boldsymbol{s}) \; d\nu \; d\Omega \; dt. \tag{11}$$

8.2 Einstein Coefficients

The three coefficients α_n^m, β_m^n, and β_n^m, describing the probabilities of the three possible transitions:

$$\begin{aligned} df_{sp} &= \alpha_n^m \, d\nu \, d\Omega \, dt, \\ df_{ab} &= \beta_m^n \, u_\nu(\boldsymbol{s}) \, d\nu \, d\Omega \, dt, \\ df_{st} &= \beta_n^m \, u_\nu(\boldsymbol{s}) \, d\nu \, d\Omega \, dt, \end{aligned} \tag{12}$$

are called the "Differential Einstein Coefficients". They are usually isotropic, i.e. they do not depend on the direction of propagation of radiation.

Einstein originally described the transition probabilities in the following form, for the case of an isotropic radiation field, and with the particles at rest:

$$\begin{aligned} dW_{sp} &= A_n^m \, dt, \\ dW_{ab} &= B_m^n U_\nu \, dt, \\ dW_{st} &= B_n^m U_\nu \, dt, \end{aligned} \tag{13}$$

where $U_\nu = \oint u_\nu(\boldsymbol{s}) \; d\Omega$ is the spectral energy density (in units of J m^{-3} Hz^{-1}). The coefficients A_n^m, B_m^n, and B_n^m, are called the "Einstein Coefficients". In such a case, the spectral lines due to the transitions between discrete energy levels must be monochromatic lines having no Doppler broadening, since the particles are at rest. If we introduce $f(\nu)$ as the probability distribution of frequency within a spectral line in a real interstellar medium in motion, the two sets of coefficients are related to each other, as follows:

$$\begin{aligned} \alpha_n^m &= \frac{A_n^m f(\nu)}{4\pi}, \\ \beta_m^n &= B_m^n \, f(\nu), \\ \beta_n^m &= B_n^m \, f(\nu). \end{aligned} \tag{14}$$

8.3 Number Density of Photons

Let the number densities of particles (number of particles per unit volume) in the states Z_m and Z_n be n_m and n_n, respectively. Then the number density of photons emitted by the $Z_n \to Z_m$ transition into the solid angle $d\Omega$ around the direction -$\boldsymbol{s}$, within the bandwidth $d\nu$, during the time interval dt, is equal to:

$$n_n(df_{sp} + df_{st}) = n_n(\alpha_n^m + \beta_n^m \; u_\nu) \; d\nu \; d\Omega \; dt.$$

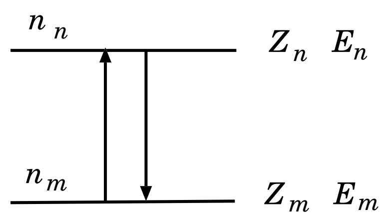

Figure 18: Number densities of particles in the two energy states.

On the other hand, the number density of photons in the same solid angle $d\Omega$, and the same bandwidth $d\nu$, absorbed by the $Z_m \rightarrow Z_n$ transition during the time interval dt, is equal to:

$$n_m df_{ab} = n_m \beta_m^n u_\nu \; d\nu \; d\Omega \; dt.$$

The differential changes in the number density of photons per unit solid angle around -$\boldsymbol{s}$, and per unit bandwidth around $\nu_{mn} = (E_n - E_m)/h$, in the course of the absorption and emission is now given by:

$$dn_p(\boldsymbol{s}, \nu) \; d\nu \; d\Omega = \{-n_m \beta_m^n u_\nu + n_n \left[\alpha_n^m + \beta_n^m u_\nu(\boldsymbol{s})\right]\} d\nu \; d\Omega \; dt.$$

Therefore, the time variation of the number density of photons is described by the following equation (Figure 19):

$$\frac{dn_p(\boldsymbol{s}, \nu)}{dt} = (n_n \beta_n^m - n_m \beta_m^n) u_\nu(\boldsymbol{s}) + n_n \alpha_n^m. \tag{15}$$

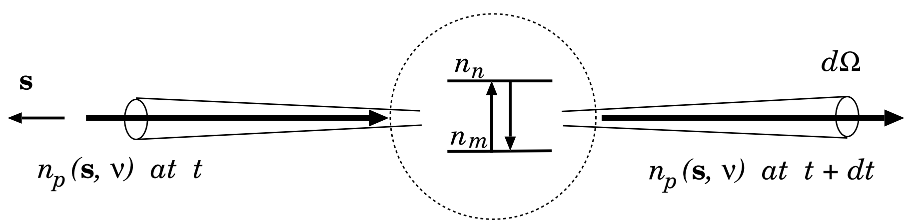

Figure 19: Time variation of the number density of photons.

9 Blackbody Radiation

We now consider the case when the radiation and matter are in thermodynamic equilibrium. Then, we have the following:

1. Stationary conditions:
   The number of transitions $Z_m \to Z_n$ must be equal to the number of opposite transitions $Z_n \to Z_m$. Requiring this stationarity in equation (15), we have:
$$n_m \beta_m^n u_\nu(\boldsymbol{s}) = n_n[\alpha_n^m + \beta_n^m u_\nu(\boldsymbol{s})]. \tag{16}$$

2. Boltzmann distribution:
   The probability P_n for a particle to be in a state Z_n, with energy level E_n, is given by the formula:
$$P_n = g_n e^{-\frac{E_n}{kT}}, \tag{17}$$
   where $k = 1.381 \times 10^{-23}$ J K^{-1} is the Boltzmann constant, T is the absolute temperature of the medium in Kelvin (K), and g_n is the statistical weight (reflecting in particular the degree of degeneracy) of the state Z_n.

If we denote the number density of all particles as n, the ratio n_n/n must be equal to the probability P_n (at least in the statistical sense). Therefore, we have
$$\frac{n_m}{n} = g_m e^{-\frac{E_m}{kT}}, \tag{18}$$
and
$$\frac{n_n}{n} = g_n e^{-\frac{E_n}{kT}}. \tag{19}$$
Inserting equations (18) and (19) into equation (16), we obtain
$$e^{-\frac{E_m}{kT}} g_m \beta_m^n u_\nu(\boldsymbol{s}) = e^{-\frac{E_n}{kT}} g_n[\alpha_n^m + \beta_n^m u_\nu(\boldsymbol{s})]. \tag{20}$$
Einstein discussed the implications of this equation, as follows:

1. The energy density per unit solid angle of the thermal radiation must tend to infinity ($u_\nu(\boldsymbol{s}) \to \infty$) when the temperature of the medium tends to infinity ($T \to \infty$) in equation (20). Hence, we obtain
$$g_m \beta_m^n = g_n \beta_n^m. \tag{21}$$
   Consequently, equation (20) becomes
$$(e^{\frac{E_n - E_m}{kT}} - 1)\beta_n^m u_\nu(\boldsymbol{s}) = \alpha_n^m. \tag{22}$$
   If we take into account the relation $h\nu = E_n - E_m$ (hereafter, we denote $\nu_{mn} = \nu$ for simplicity), the energy density per unit solid angle can be expressed as
$$u_\nu = \frac{\alpha_n^m}{\beta_n^m} \frac{1}{e^{\frac{h\nu}{kT}} - 1}. \tag{23}$$

Henceforth, we omit the $\boldsymbol{s}$ dependence in u_ν, since the RHS of equation (23) does not depend on any specific direction, as expected from the isotropic nature of thermal radiation.

2. The energy density per unit solid angle u_ν must follow the well-known Rayleigh–Jeans radiation law:

$$u_\nu = \frac{2\nu^2}{c^3} kT, \tag{24}$$

in the classical limit $h\nu \ll kT$. Therefore, we must require in equation (23)

$$\frac{\alpha_n^m}{\beta_n^m} = \frac{2h\nu^3}{c^3}. \tag{25}$$

The above discussions thus lead to Planck's formula of blackbody radiation:

$$u_\nu = \frac{2h\nu^3}{c^3} \frac{1}{e^{\frac{h\nu}{kT}} - 1}\ . \tag{26}$$

For the intensity I_ν, we obtain

$$I_\nu = c u_\nu = \frac{2h\nu^3}{c^2} \frac{1}{e^{\frac{h\nu}{kT}} - 1}, \tag{27}$$

(see Figure 20). For the energy density U_ν, we have

$$U_\nu = \oint u_\nu d\Omega = 4\pi u_\nu = \frac{8\pi h\nu^3}{c^3} \frac{1}{e^{\frac{h\nu}{kT}} - 1}\ . \tag{28}$$

9.1 Two Extreme Cases of the Planck Spectrum

- Rayleigh–Jeans region ($h\nu \ll kT$, and hence $e^{\frac{h\nu}{kT}} \simeq 1 + \frac{h\nu}{kT}$):

$$I_\nu = \frac{2\nu^2}{c^2} kT. \tag{29}$$

  Note that thermal radiation in the radio frequency range is mostly in the Rayleigh–Jeans region.

- Wien region ($h\nu \gg kT$):

$$I_\nu = \frac{2h\nu^3}{c^2} e^{-\frac{h\nu}{kT}}. \tag{30}$$

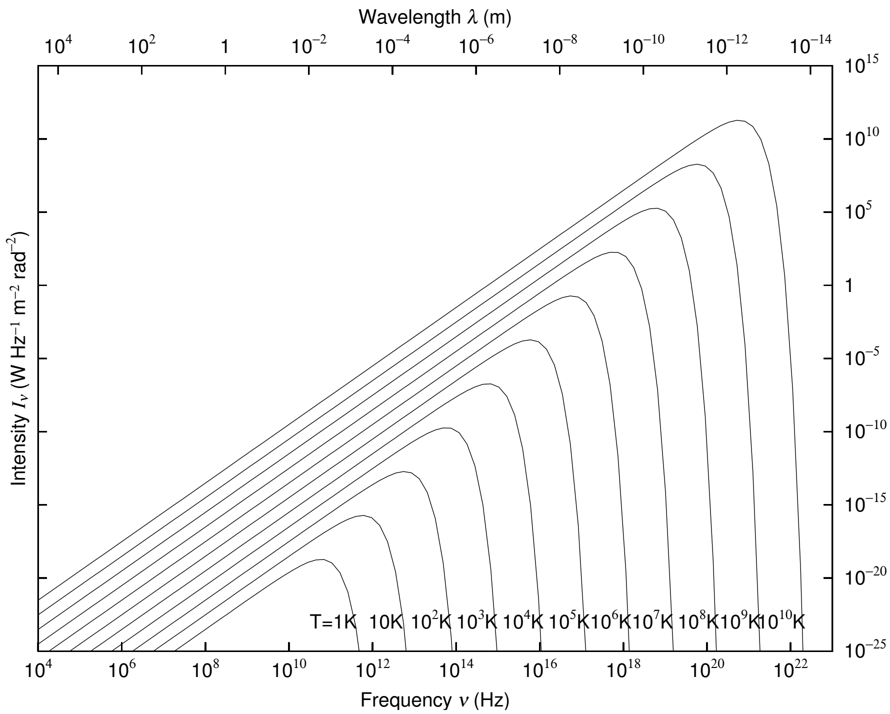

Figure 20: Planck spectrum of black body radiation. Each curve corresponds to a certain absolute thermodynamic temperature value.

9.2 Wien's Law

The peak frequency of the Planck spectrum at a given temperature T is

$$\nu_{max} \text{ (in Hz)} = 5.8789 \times 10^{10} T \text{ (in K)}. \tag{31}$$

One can easily derive this law by equating to zero the derivative of the intensity I_ν with respect to frequency ν, in equation (27).

This, Wien's law, explains why stars with higher temperatures appear bluer, and those with lower temperatures appear redder. Conversely, astronomers infer one of the most important physical parameters of stars, the surface temperature, from measuring their color.

Can we observe the peak of the thermal blackbody spectrum in the radio region?

- No hope for thermal radiation from a stellar surface, or from a fairly warm interstellar cloud.
- For submillimeter waves at around 500 GHz (which are still regarded as radio waves), we can see the peak if the temperature of the medium is below 10 K ($T \leq 10$ K).
- For example, the cosmic background radiation with $T \simeq 2.7$ K has its peak at around 170 GHz.

9.3 Spectral Indices of Thermal Continuum Radio Sources

We now understand why the spetral indicies α ($\mathcal{S}_\nu \propto \nu^{-\alpha}$) of thermal continuum radio sources like the Moon, the quiet Sun, and the left half portion of the spectrum of Orion nebula, are all close to -2 ($\alpha \simeq -2$). This is because thermal continuum sources mostly show Rayleigh–Jeans spectra, $I_\nu = \frac{2\nu^2}{c^2} kT$, in the radio region.

9.4 Stars are Faint and Gas Clouds are Bright in the Radio Sky

According to the Planck spectrum, the intensity of a hotter black body is always stronger than the intensity of a colder body, for any frequency range. On the other hand, the flux density S_ν, which we directly detect with our radio telescopes, is proportional to the product of the intensity I_ν and the solid angle of the radio source Ω ($\mathcal{S}_\nu \propto I_\nu \Omega$). While the surface temperatures

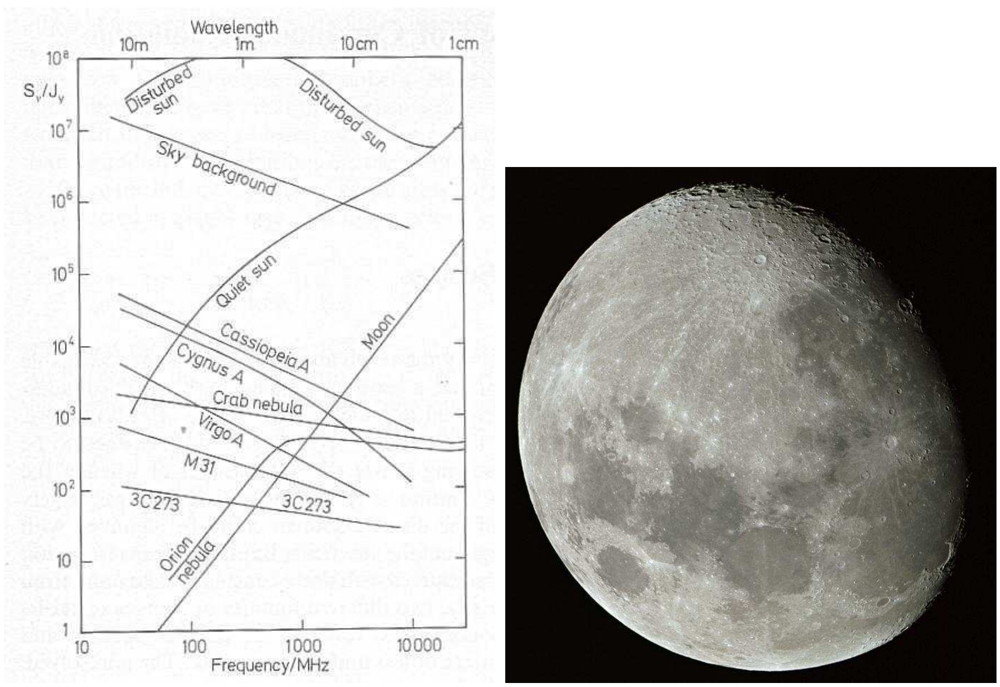

Figure 21: Spectra of continuum radio sources (Kraus, 1986; left), and an optical image of the Moon (right). Do we see such a halfmoon image in radio waves?

of ordinary stars are fairly high (several thousands to several tens of thousand Kelvin), their solid angles, which are inversely proportional to their squared distances, are very small. For example, if we were to put the Sun at the distance of the nearest star, which is about 3 light years, or 1 parsec, the Sun's angular diameter would be only $\simeq 0.01$ arcsecond! As a result, the flux density 5×10^6 Jy of the quiet Sun at 10 GHz (see Figure 2) would be reduced down to 125 μJy at the distance of the nearest star. On the contrary, the interstellar gas clouds, as cold as tens to hundreds of Kelvin, still clearly shine in the radio sky, because their angular diameters are as large as minutes to degrees of arc. For example, Figure 2 shows that the flux density of the Orion Nebula is about 500 Jy at around 500 MHz.

9.5 Stefan–Boltzmann Law

The total intensity $I(T)$ of the thermal radiation from a black body of temperature T, over the entire frequency range, is given by

$$I(T) = \int_0^\infty I_\nu d\nu = \int_0^\infty \frac{2h\nu^3}{c^2} \frac{1}{e^{\frac{h\nu}{kT}} - 1} d\nu = \frac{1}{\pi} \sigma T^4, \tag{32}$$

where σ is the Stefan–Boltzmann constant:

$$\sigma = \frac{2\pi^5 k^4}{15 c^2 h^3} = 5.6697 \times 10^{-8} \quad \mathrm{W\ m^{-2}\ K^{-4}}.$$

Equation (32) can be derived using the integration formula:

$$\int_0^\infty \frac{2x^{2n-1}}{e^{2\pi x} - 1} dx = \frac{\mathcal{B}_n}{2n} \quad , \tag{33}$$

where $\mathcal{B}_n$ is the n-th Bernoulli number, and $\mathcal{B}_2 = 1/30$.

9.6 Total Blackbody Radiation from a Star or a Gas Cloud

The power flux density $S_\star$, at a surface of a blackbody, which is the power over the entire frequency range through a cross section of unit area of the surface (Figure 22), is given by the equation:

$$\begin{aligned} S_\star &= \int_0^\infty \mathcal{S}_\nu \, d\nu = \int_0^\infty \int_0^{\frac{\pi}{2}} \int_0^{2\pi} I_\nu \ \cos\theta \sin\theta \, d\phi \, d\theta \, d\nu \\ &= I(T) \int_0^{\frac{\pi}{2}} \int_0^{2\pi} \cos\theta \sin\theta \, d\phi \, d\theta = \pi \, I(T) = \sigma T^4. \end{aligned} \tag{34}$$

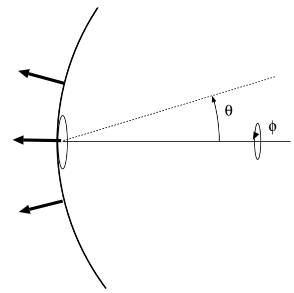

Figure 22: Thermal radiation from a surface of a black body.

Therefore, the total power $\mathcal{F}$ of the blackbody radiation from a spherical star with radius R is equal to:

$$\mathcal{F} = 4\pi R^2 S_\star = 4\pi R^2 \sigma T^4.$$

The power flux density of the thermal radiation which we receive from a star or a cloud of solid angle Ω, surface temperature T, and distance r, is from equation (32):

$$\mathcal{S} = \Omega\ I = \frac{\Omega \sigma T^4}{\pi}\ ,$$

which, for the spherically symmetric case where $\Omega = \pi R^2/r^2$, is reduced to

$$\mathcal{S} = \frac{R^2}{r^2}\sigma T^4 = \frac{R^2}{r^2} S_\star = \frac{\mathcal{F}}{4\pi r^2}\ ,$$

as expected.

9.7 Universality of the Relationship among Einstein's Coefficients

We derived equations (21) and (25), giving the following relationships among Einstein's coefficients:

$$\begin{aligned} g_m \beta_m^n &= g_n \beta_n^m, \\ \frac{\alpha_n^m}{\beta_n^m} &= \frac{2h\nu^3}{c^3}, \end{aligned}$$

or, equivalently,

$$\begin{aligned} g_m B_m^n &= g_n B_n^m, \\ \frac{A_n^m}{B_n^m} &= \frac{8\pi h\nu^3}{c^3}, \end{aligned}$$

by assuming thermodynamic equilibrium. However, the resulting equations above do not contain any quantity characteristic of thermodynamics. This means that the equations must hold universally, irrespective of whether the condition of thermodynamic equilibrium is fulfilled. These relationships are determined by the microscopic interactions between a photon and a particle, and are not influenced by the environment (temperature, pressure, ... etc.). We obtained the relationships under the assumption of thermodynamic equilibrium, where it is most easily derived. Analogously, if you find a big hole in a road in daytime, you would assume that the hole still exists at night, when you cannot see it well.

9.8 Another Important Quantity in Radio Astronomy

Brightness Temperature

The brightness temperature T_B of a source with monochromatic intensity (or surface brightness) I_ν, is a quantity which is defined by the equation:

$$T_B = \frac{c^2}{2k\nu^2} I_\nu. \tag{35}$$

This is a quantity with the dimension of temperature obtained by a 'forced' application of the Rayleigh–Jeans formula to the radiation from any radio source. If the radiation comes from a sufficiently hot ($T \gg 10$ K) thermal source, without noticeable absorption or additional emission along the propagation path, the brightness temperature must correspond to the physical temperature of the source. If the source is non–thermal, the brightness temperature has no relevance to any real temperature. For example, for some maser sources, the brightness temperature could be as high as 10^{14} K, although the physical temperature values of the 'masing' (i.e. maser–emitting) gas clouds are only several hundreds of Kelvin. The word 'brightness temperature' is a jargon term which is used only, but quite frequently, in radio astronomy.

10 Radiative Transfer

10.1 Phenomenological Derivation of the Radiative Transfer Equation

Radiative transfer theory describes how the intensity varies as radiation propagates in an absorbing and/or emitting medium. The equation of radiative transfer can be phenomenologically derived as follows:

Let the intensity I_ν change by dI_ν due to absorption and emission as the radiation passes through an infinitesimal distance dl (Figure 23). The

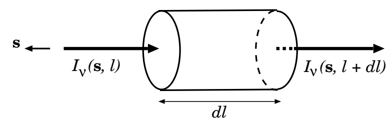

Figure 23: Radiative transfer through a cylinder of infinitesimal length.

variation can be described as a sum of two contributions: one due to the absorption $-\kappa_\nu I_\nu dl$, and one due to the emission $\epsilon_\nu dl$, where κ_ν and ϵ_ν are the following frequency–dependent coefficients:

$$\begin{array}{lll} \kappa_\nu & : \text{ opacity} & \text{m}^{-1}, \\ \epsilon_\nu & : \text{ emissivity} & \text{W m}^{-3}\text{ Hz}^{-1}\text{ sr}^{-1}. \end{array}$$

We then obtain the radiative transfer equation in the following form:

$$\frac{dI_\nu}{dl} = -\kappa_\nu I_\nu + \epsilon_\nu \ . \tag{36}$$

10.2 Derivation of the Radiative Transfer Equation from Einstein's Elementary Quantum Theory of Radiation

Equation (36) can also be derived from equation (15) obtained in the discussion of Einstein's elementary quantum theory of radiation:

$$\frac{dn_p(\boldsymbol{s},\nu)}{dt} = (n_n\beta_n^m - n_m\beta_m^n)u_\nu(\boldsymbol{s}) + n_n\alpha_n^m,$$

where n_p is the number density of photons per unit solid angle and per unit frequency bandwidth, u_ν is the spectral energy density per unit solid angle, n_m and n_n are the number densities of the particles in states Z_m and Z_n, and α_n^m, β_n^m and β_m^n are Einstein's differential coefficients. In fact, using the relations:

$$\begin{aligned} u_\nu(\boldsymbol{s}) &= h\nu n_p(\boldsymbol{s},\nu), \\ I_\nu(\boldsymbol{s}) &= cu_\nu(\boldsymbol{s}), \\ dl &= cdt \ , \end{aligned}$$

we can transform equation (15) to:

$$\frac{dI_\nu}{dl} = -(n_m\beta_m^n - n_n\beta_n^m)\frac{h\nu}{c}I_\nu + h\nu n_n\alpha_n^m. \tag{37}$$

Therefore, if we denote

$$\begin{array}{rcll} \kappa_\nu & = & (n_m\beta_m^n - n_n\beta_n^m)\frac{h\nu}{c} & : \text{absorption and induced emission,} \\ \epsilon_\nu & = & h\nu n_n\alpha_n^m & : \text{spontaneous emission,} \end{array} \tag{38}$$

equation (37) is reduced to the radiative transfer equation (36).

Role of the induced emission

In the resulting radiative transfer equation:

$$\frac{dI_\nu}{dl} = -\kappa_\nu I_\nu + \epsilon_\nu \ ,$$

the opacity κ_ν now contains not only the contribution of simple absorption but also that of induced emission, as we see in equation (38). According to equation (21) obtained by Einstein:

$$g_m\beta_m^n = g_n\beta_n^m,$$

we can now express the opacity κ_ν as

$$\kappa_\nu = (n_m - \frac{g_m}{g_n}n_n)\beta_m^n\frac{h\nu}{c}. \tag{39}$$

If we consider the simple case where the statistical weights of the two states are equal to each other ($g_m = g_n$), the above equation (39) reduces to

$$\kappa_\nu = (n_m - n_n)\beta_m^n\frac{h\nu}{c}. \tag{40}$$

It is worthy to note that the opacity takes on a **negative** value when the number density of the particles in the higher energy level is larger than that at the lower level ($n_n > n_m$).

10.3 The Simplest Solutions of Radiative Transfer Equation

Let us solve the radiative transfer equation (36):

$$\frac{dI_\nu}{dl} = -\kappa_\nu I_\nu + \epsilon_\nu \ ,$$

under the following simple conditions.

1. **When** $\kappa_\nu = 0$,
   the solution of equation (36) is just a simple integral:
$$I_\nu(l) = I_\nu(0) + \int_0^l \epsilon_\nu(l')dl' \ . \tag{41}$$

2. **When** $\epsilon_\nu = 0$,
   the solution is an exponential function:
$$I_\nu(l) = I_\nu(0) e^{-\int_0^l \kappa_\nu(l')dl'} \ . \tag{42}$$

   If the medium is homogeneous, i.e. $\kappa_\nu =$ constant everywhere, then
$$I_\nu(l) = I_\nu(0) e^{-\kappa_\nu l} \ . \tag{43}$$

   Here,
   $\kappa_\nu > 0$ (positive opacity) implies an exponential decay, which arises from ordinary absorption, and
   $\kappa_\nu < 0$ (negative opacity) implies an exponential growth, which arises from maser amplification.

Maser Amplification

When the number density n_n of particles at a higher energy level E_n is, for some reason, larger than n_m at a lower energy level E_m (such a situation is called a "population inversion"), the opacity becomes negative ($\kappa_\nu < 0$), and the radiation of the frequency corresponding to the transition between the energy levels is exponentially amplified along the initial direction of propagation (Figure 24). Since this amplification is due to induced (or stimulated) emission, it is called a "MASER" (Microwave Amplification of Stimulated Emission of Radiation). The same mechanism in the visible light region of electromagnetic waves is called the "LASER" (Light Amplification of Stimulated Emission of Radiation).

If the thermal equilibrium condition is fulfilled in the gas medium, the Boltzmann distribution always ensures $n_n < n_m$, and no maser amplification can occur. Therefore, maser emission is essentially non–thermal. We need some "pumping mechanism" which realizes the population inversion in order to get the maser mechanism to work. In actual interstellar space, strong infrared radiation from stars, or collisions of gas molecules, may serve as a pumping mechanism.

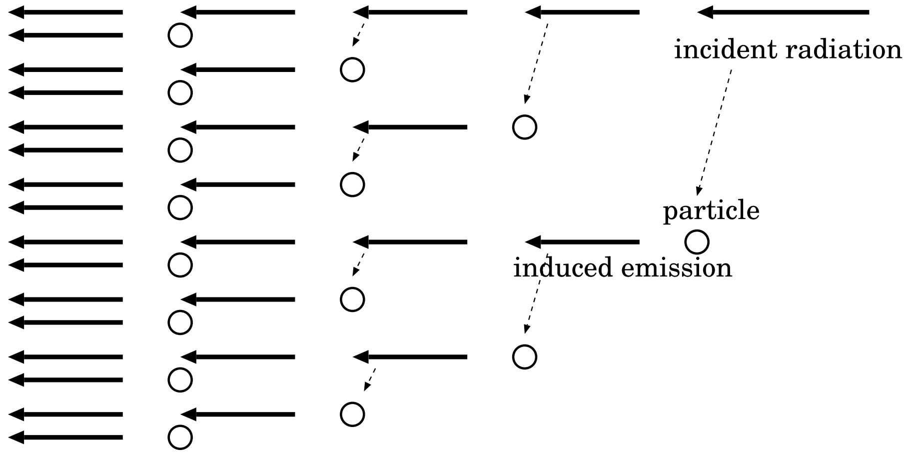

Figure 24: A schematic view of maser amplification. Induced emission causes new induced emission, initiating an "avalanche" of maser emission photons all traveling in a common direction parallel to the incident photon.

Usually, masers are strong radio sources. For example, the brightness temperature of some H_2O masers is as high as 10^{14} K.

3. **In the purely thermal equilibrium case**,
we obtain from the detailed balance:

$$-\kappa_\nu I_\nu + \epsilon_\nu = 0, \quad \text{and therefore} \quad I_\nu = \frac{\epsilon_\nu}{\kappa_\nu},$$

and from the Planck spectrum:

$$I_\nu = \mathcal{B}_\nu(T) \equiv \frac{2h\nu^3}{c^2} \frac{1}{e^{\frac{h\nu}{kT}} - 1} \ ,$$

where $\mathcal{B}_\nu(T)$ is defined to be the Planck function. From the above equations, we have a relationship between the emissivity and opacity, which is called Kirchoff's law:

$$\frac{\epsilon_\nu}{\kappa_\nu} = \mathcal{B}_\nu(T) \ . \tag{44}$$

4. **Local thermodynamic equilibrium (LTE)**
In a fairly wide range of real circumstances in interstellar gas media, and in laboratory conditions, at a given temperature T, there is the case when Kirchoff's law $\epsilon_\nu/\kappa_\nu = \mathcal{B}_\nu(T)$ holds to a good approximation, but the radiation intensity I_ν is **not** equal to the Planck function

$\mathcal{B}_\nu(T)$ at temperature T. Such a case is called "local thermodynamic equilibrium", denoted by "LTE".

In LTE, the radiative transfer equation reduces to

$$\frac{dI_\nu}{dl} = -\kappa_\nu [I_\nu - \mathcal{B}_\nu] \ . \tag{45}$$

Then, introducing the "optical depth" τ_ν, which satisfies

$$d\tau_\nu = -\kappa_\nu dl, \tag{46}$$

we can further transform equation (45) to

$$\frac{dI_\nu}{d\tau_\nu} = I_\nu - \mathcal{B}_\nu(T) \ . \tag{47}$$

Suppose we have an emitting and absorbing gas medium confined within a finite linear extent l_0, and we consider the radiation coming from the outside ($l < 0$, see Figure 25). The optical depth τ_ν is chosen to be equal to $\tau_\nu(0)$ at $l = 0$, and to 0 at $l = l_0$.

The solutions to equation (47) are:

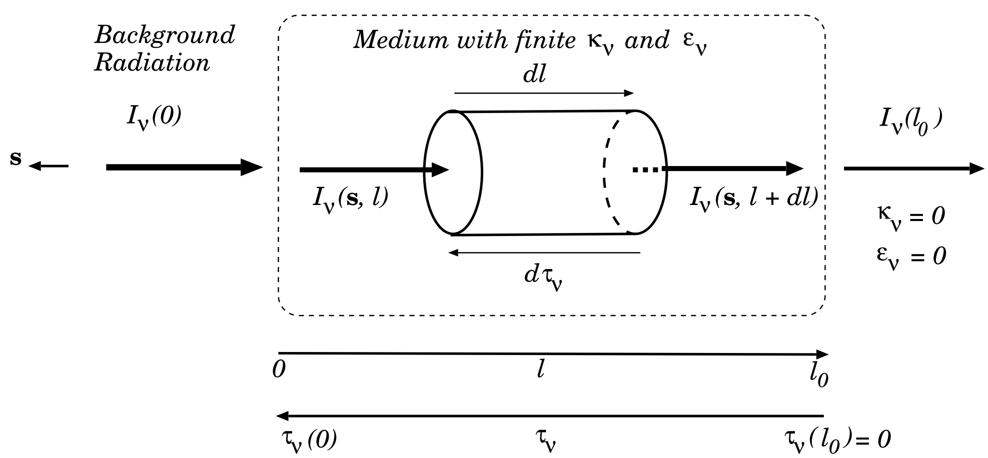

Figure 25: Radiative transfer in LTE and optical depth.

within the medium ($0 \leq l \leq l_0$):

$$I_\nu(l) = I_\nu(0) e^{\tau_\nu - \tau_\nu(0)} + e^{\tau_\nu} \int_{\tau_\nu}^{\tau_\nu(0)} \mathcal{B}_\nu(T(\tau')) e^{-\tau'} d\tau', \tag{48}$$

and **outside the medium** ($l_0 \leq l$):

$$I_\nu(l) = I_\nu(l_0) = I_\nu(0)e^{-\tau_\nu(0)} + \int\limits_0^{\tau_\nu(0)} \mathcal{B}_\nu(T(\tau'))e^{-\tau'}d\tau' \ , \qquad (49)$$

where $I_\nu(0)$ is the incoming background radiation.

5. **LTE and isothermal medium**
If the medium is isothermal ($T(\tau') = T = const$), the solutions are:
within the medium ($0 \leq l \leq l_0$):

$$I_\nu(l) = I_\nu(0)e^{\tau_\nu - \tau_\nu(0)} + \mathcal{B}_\nu(T)(1 - e^{\tau_\nu - \tau_\nu(0)}), \qquad (50)$$

and **outside the medium** ($l_0 \leq l$):

$$I_\nu(l) = I_\nu(l_0) = I_\nu(0)e^{-\tau_\nu(0)} + \mathcal{B}_\nu(T)(1 - e^{-\tau_\nu(0)}) \ . \qquad (51)$$

Note that $I_\nu \to \mathcal{B}_\nu(T)$ when $\tau_\nu(0) \to \infty$ in the above equations. This means that **thermal radiation becomes blackbody radiation reflecting the temperature of the medium when, and only when, the medium is completely opaque**.

If we denote the intensity I_ν in terms of the brightness temperature T_B, and adopt the Rayleigh–Jeans approximation for $\mathcal{B}_\nu(T)$:

$$I_\nu = \frac{2\nu^2}{c^2}kT_B \quad \text{and} \quad \mathcal{B}_\nu(T) = \frac{2\nu^2}{c^2}kT \ ,$$

the equation (51) for the solution of the radiative transfer equation outside the medium can be described by

$$T_B(l) = T_B(0)e^{-\tau_\nu(0)} + T(1 - e^{-\tau_\nu(0)}) \ . \qquad (52)$$

10.4 What is LTE?

How can the Kirchoff law $\epsilon_\nu/\kappa_\nu = \mathcal{B}_\nu(T)$ be satisfied, even though the intensity of the radiation is not blackbody?

The opacity and emissivity are expressed in terms of Einstein's differential coefficients, as we saw in equation (38)

$$\begin{aligned} \kappa_\nu &= (n_m\beta_m^n - n_n\beta_n^m)\frac{h\nu}{c}, \\ \epsilon_\nu &= h\nu n_n\alpha_n^m. \end{aligned}$$

Taking into account Einstein's relations among the differential coefficients in equations (21) and (25):

$$\begin{aligned} g_m \beta_m^n &= g_n \beta_n^m, \\ \frac{\alpha_n^m}{\beta_n^m} &= \frac{2h\nu^3}{c^3}, \end{aligned}$$

we can express the emissivity–opacity ratio as

$$\frac{\epsilon_\nu}{\kappa_\nu} = \frac{1}{\frac{n_m}{n_n}\frac{g_n}{g_m} - 1} \frac{2h\nu^3}{c^2}\ , \tag{53}$$

using equation (39). Obviously, the right hand side of equation (53) becomes the Planck function if the Boltzmann distribution

$$P_n = \frac{n_n}{n} = g_n e^{-\frac{E_n}{kT}},$$

(equation (17)) holds, and hence

$$\frac{n_m}{n_n}\frac{g_n}{g_m} = e^{\frac{h\nu}{kT}}.$$

Therefore, we can interpret LTE as a physical situation where the Boltzmann distribution is established among the particles in a medium due, for example, to their mutual collisions, but in which the radiation is still not in equilibrium with the particles.

10.5 Spectrum of the Orion Nebula

Now we are in a position to interpret qualitatively the bend in the spectrum of the Orion Nebula, as shown in Figures 2 and 26. If we neglect the contribution of the background radiation in the solution of the radiative transfer equation in the isothermal LTE case (equation (51)), the intensity is given by

$$I_\nu = \mathcal{B}_\nu(T)(1 - e^{-\tau_\nu(0)}).$$

Therefore, the bending can be explained if the nebula is completely opaque ($\tau_\nu(0) \gg 1$) at low frequencies, but not at high frequencies. In the higher frequency range, the radiation no longer shows the blackbody spectrum. But this type of radiation is still usually included in the category of thermal radiation, since this is caused by the thermal motion of free electrons in the plasma gas, and tends to have the blackbody (Planck) spectrum in the completely opaque limit.

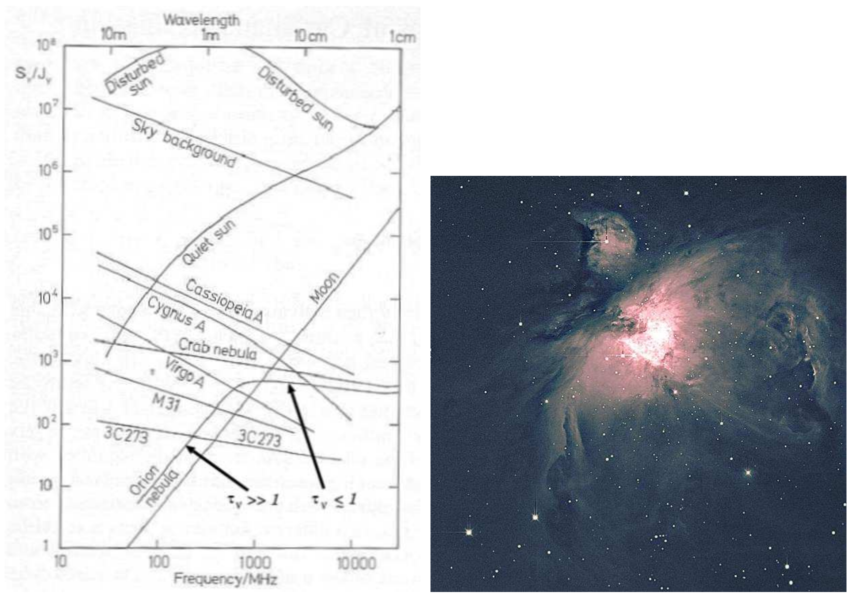

Figure 26: Interpretation of the spectrum of the Orion Nebula. Left panel is from Kraus (1986).

11 Synchrotron Radiation

Synchrotron radiation is a typical example of non-thermal radiation caused by the high–speed ("relativistic") electrons in their accelerated helical motion in a magnetic field. Historically, synchrotron radiation was first discovered in 1948, as the light emitted by a particle accelerator called the "Synchrotron". Synchrotron radiation is dominant in a variety of astronomical objects, including "Active Galactic Nuclei" (AGNs), Supernova Remnants (SNRs), and solar flares (see Figure 27 as an example).

11.1 Non–Relativistic Case

In the non–relativistic case, the analog of synchrotron radiation is known as "cyclotron" or "gyro–synchrotron" radiation. In this case, the balance of the Lorentz force and the centrifugal force

$$e(\boldsymbol{v}_\perp \times \mathrm{B}) = \frac{m_0 v_\perp^2}{r},$$

gives rise to "Larmor Precession" with "gyro–frequency" ν_G:

$$\nu_G = \frac{v_\perp}{2\pi r} = \frac{1}{2\pi}\frac{eB}{m_0},$$

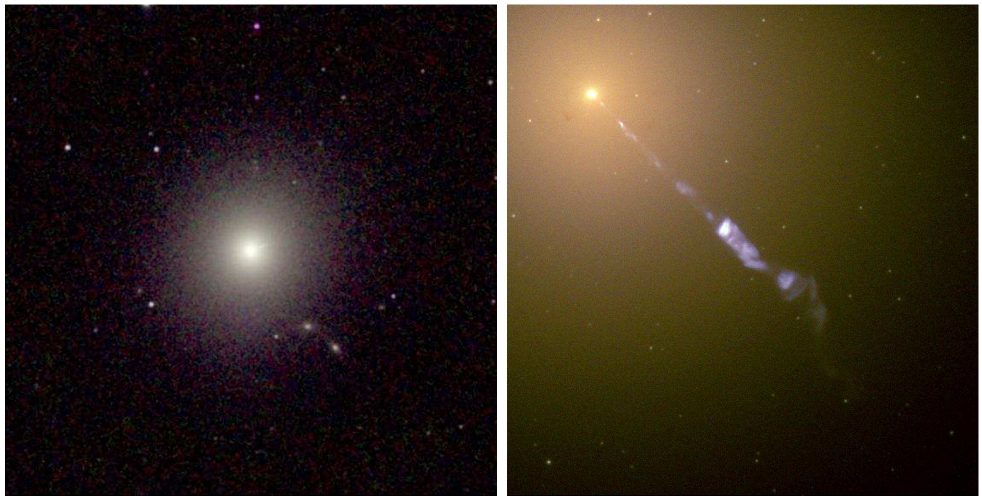

Figure 27: Many galaxies show activity in their nuclei, involving violent ejections of high–energy electrons and resultant synchrotron radiation. A nearby galaxy M87, also known as Virgo A or 3C 274 in radio astronomy, is an example. Left: Infrared image of M87 by 2 Micron All Sky Survey (2MASS). Right: Close–up view of a collimated jet by Hubble Space Telescope (HST). (Figure courtesy of NASA/IPAC Extragalactic Database (NED) operated by the Jet Propulsion Laboratory, California Institute of Technology, under contract with the National Aeronautics and Space Administration).

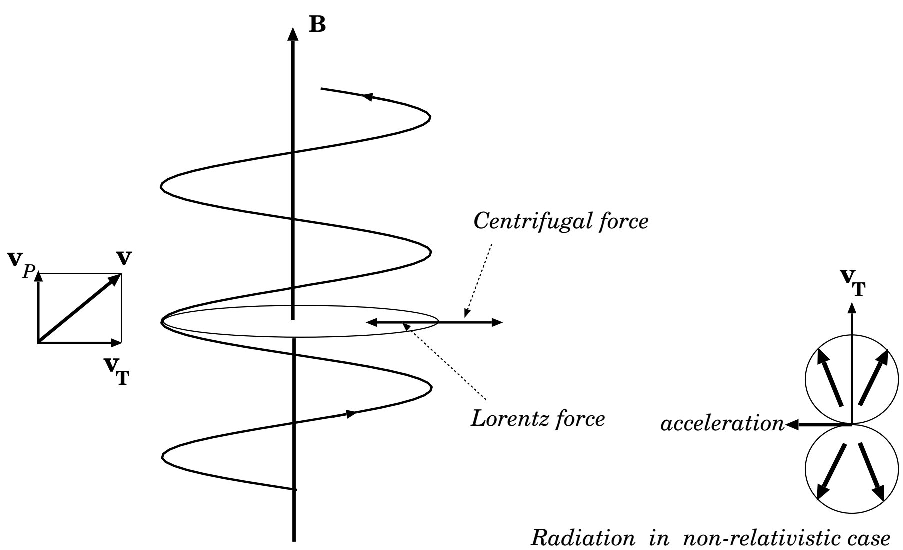

Figure 28: "Cyclotron" or "Gyro–synchrotron" radiation

where m_0, e and $\boldsymbol{v}$ are rest mass, electric charge and velocity of an electron, while $\boldsymbol{B}$ is the magnetic flux density (Figure 28).

The gyro–frequency ν_G does not depend on the velocity of the electron. Therefore, for any electron velocity, cyclotron radiation is emitted as a line at frequency ν_G, which is modulated only by the spatial and temporal variation of the magnetic field.

11.2 Relativistic Case

In the relativistic case, when the electron velocity v approaches light velocity c, the radiation from an accelerated electron is emitted almost exclusively in the direction of movement of the electron, due to the relativistic beaming effect (Figure 29). A distant observer can detect this pulse–like radiation only when the narrow beam is directed along or near the line of sight. Since the beam direction rotates around the magnetic field at high speed, the resulting high frequency pulses from a single electron produce a continuum–like spectrum, with a peak frequency ν_{max}:

$$\nu_{max} \propto \frac{\nu_G}{1 - \frac{v^2}{c^2}} \ . \tag{54}$$

The energy distribution of high–energy electrons in active regions, such as AGNs and SNRs, usually follows a power law:

$$N(E) \propto E^{-\gamma}, \tag{55}$$

where E is the energy of the electron, $N(E)$ is the number density of electrons with energy E per unit energy range, and γ is the index of the energy spectrum. Since the energy of an electron with velocity v:

$$E = mc^2 = \frac{m_0 c^2}{\sqrt{1 - \frac{v^2}{c^2}}}, \tag{56}$$

is proportional to the square root of its peak frequency ν_{max} given in equation (54) (i.e. $E \propto \nu_{max}^{1/2}$), a large number of electrons in a wide range of energy yield a compound spectrum with energy density U_ν, which is roughly given by

$$U_\nu \propto \nu^{\frac{1-\gamma}{2}} \ . \tag{57}$$

Since the index γ of the energy spectrum of high–energy electrons, as observed in the cosmic rays, is roughly $\gamma \simeq 2.4$, we can expect that the spectrum of the synchrotron radiation is approximately

$$U_\nu \propto \nu^{-0.7}. \tag{58}$$

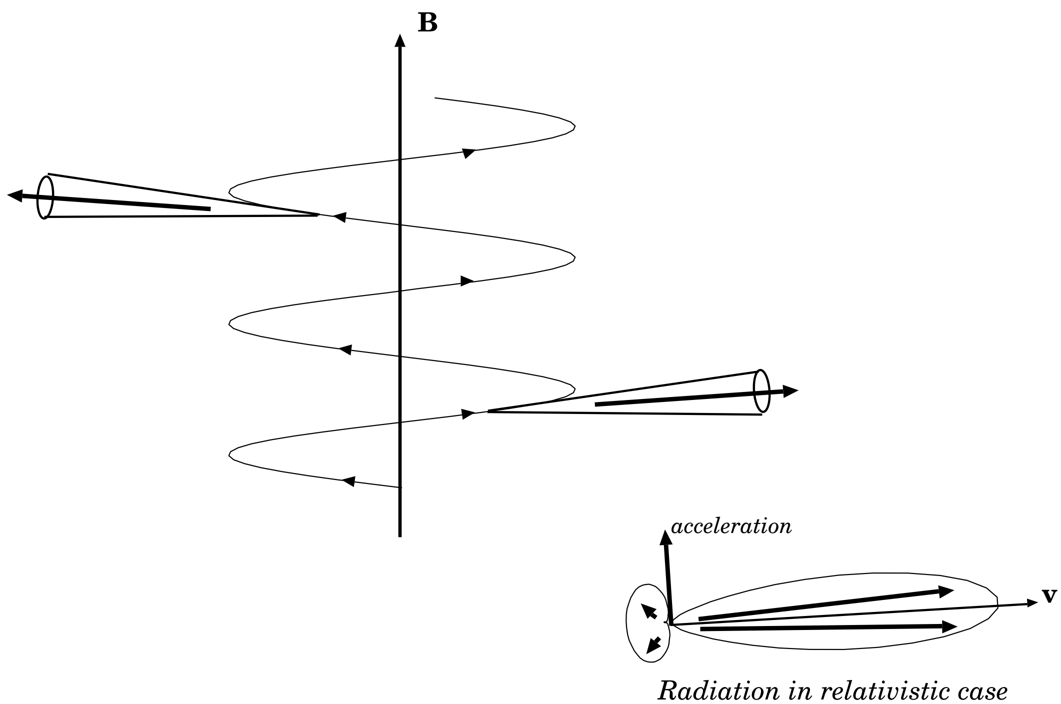

Figure 29: Synchrotron radiation from a relativistic electron.

Therefore, the spectral index ($S_\nu \propto \nu^{-\alpha}$) is around $\alpha \simeq 0.7$.

Thus, we can now explain the observed positive spectral indices of the spectra of the non–thermal sources such as Crab Nebula, Cygnus A, 3C273, the disturbed Sun, etc. (Figure 30).

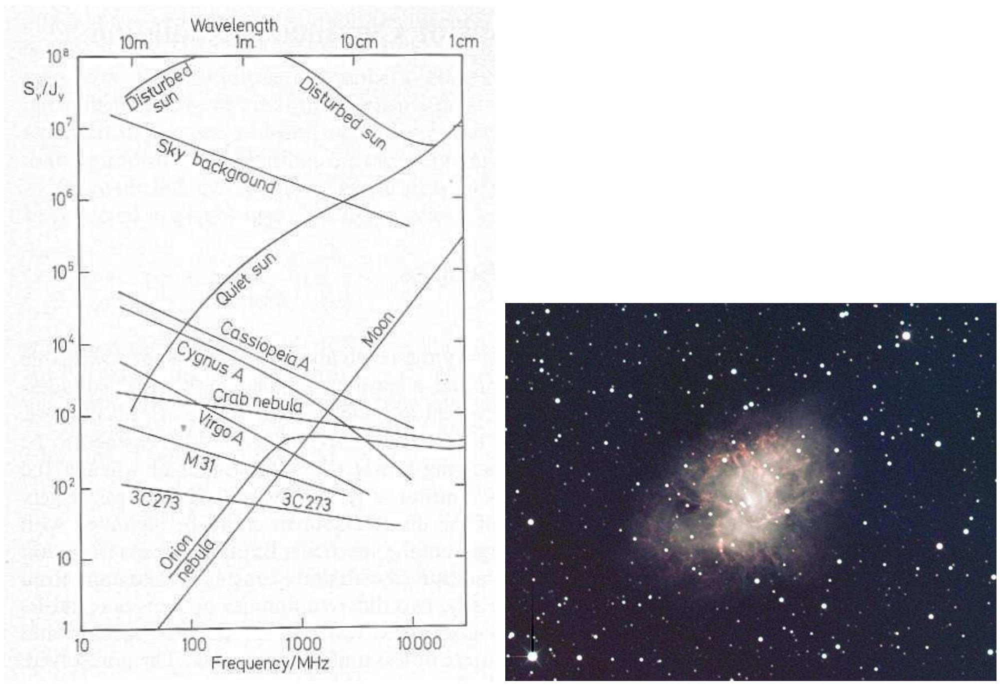

Figure 30: Spectra of continuum radio sources, including non–thermal sources with positive spectral indices (Kraus, 1986; left), and the Crab Nebula supernova remnant, a typical synchrotron radiation source.

References

Einstein, A., 1916, Zur Quantentheorie der Strahlung, *Mitt. Phys. Ges. (Zürich)*, **18**, 47–62. (This paper was also published in *Physikalishe Zeitschrift*, 1917, **18**, 121.)

Kaifu, N., Suzuki, H., Ohishi, M., Morimoto, M., and Miyaji, T., 1985, *NRO Graphic Report No.1* (Nobeyama, Japan).

Kraus, J.D., 1986, Radio Astronomy, 2nd Edition, *Cygnus–Quasar Books* (Powell, Ohio, U.S.A.).

Rohlfs, K., and Wilson, T.L., 2000, Tools of Radio Astronomy, 3rd Edition, *Springer–Verlag* (Germany).

Westerhout, G., 1958, A Survey of the Continuous Radiation from the Galactic System at a Frequency of 1390 Mc/s, *Bull. Astron. Inst. Netherlands*, **14**, 215.